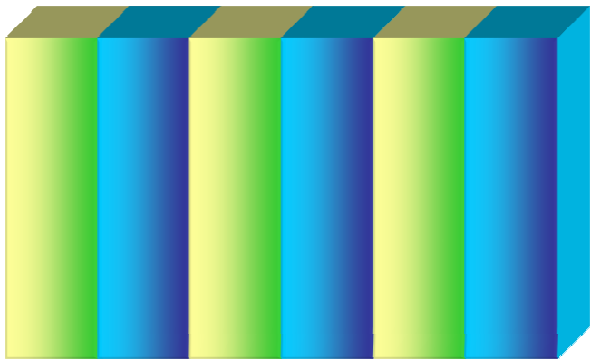


Novel phononic metamaterials for acoustic and thermal applications

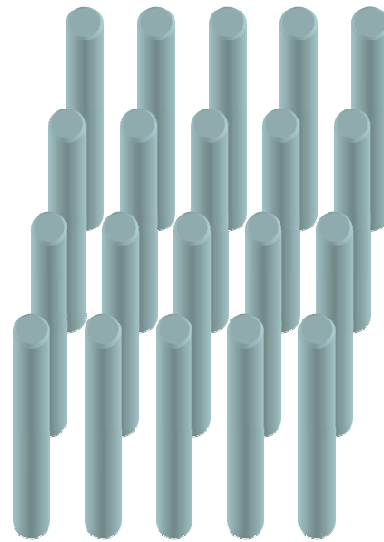
Krishna Muralidharan
Materials Science and Engineering
University of Arizona

PHONONIC METAMATERIALS

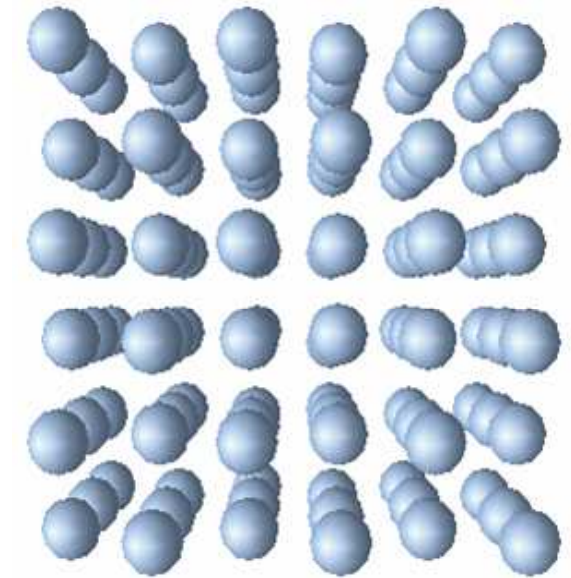
- Artificially structured composite materials whose elastic constants and density are periodic functions of the position (1D, 2D, 3D)



1D: Multilayers materials



2D: Array of cylinders of circular, square, cross section embedded in a matrix



3D: Array of spherical, cubic, ... inclusions embedded in a matrix

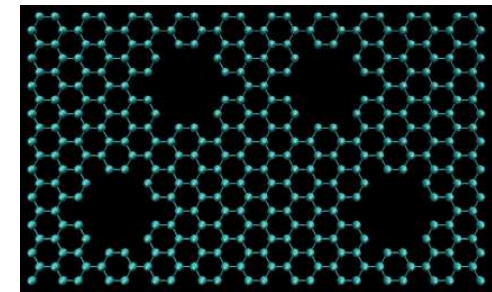
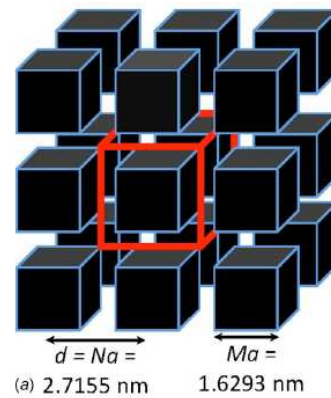
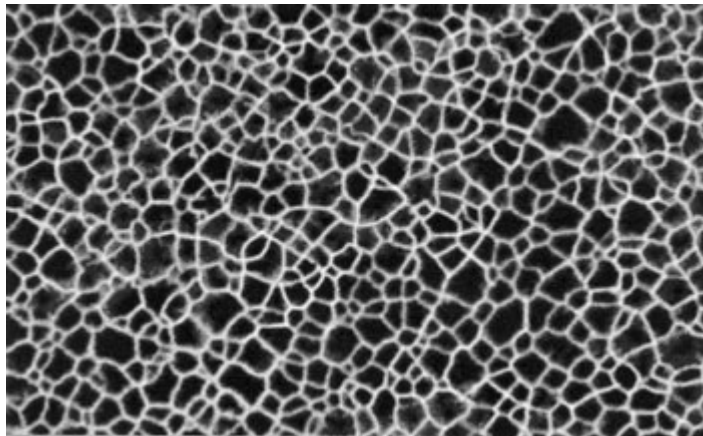
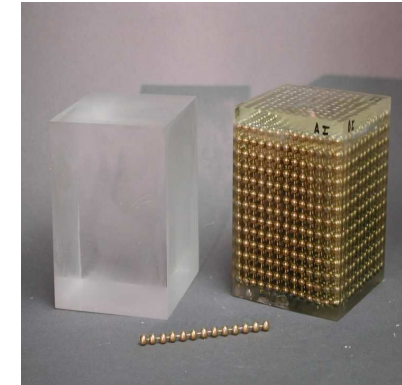
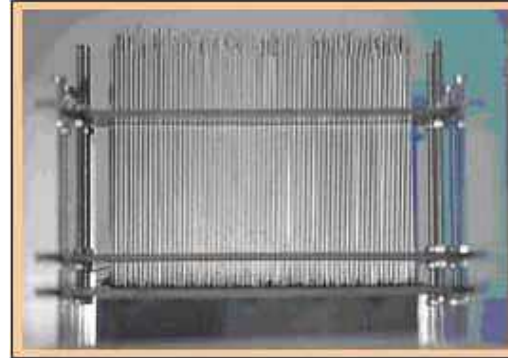
PHYSICAL PARAMETERS

 **Constituents** : Solid/solid, fluid/fluid, mixed solid/fluid composites (Parameters: longitudinal and/or transverse speeds of sound, density)

 **Composition** : $f \equiv$ filling fraction of inclusions

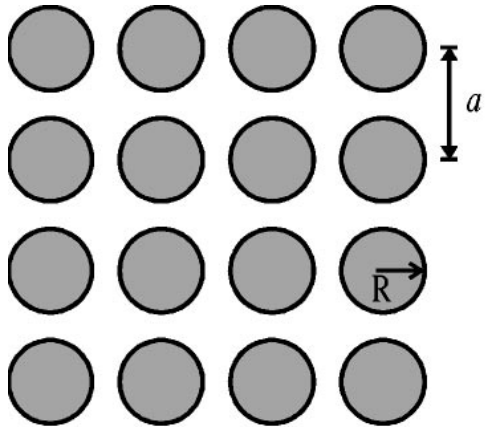
 **Structure** : Geometry (Lattices: square array, triangular lattice, boron-nitride structure,..., lattice parameter, inclusion size and geometry).

Phononic Crystals

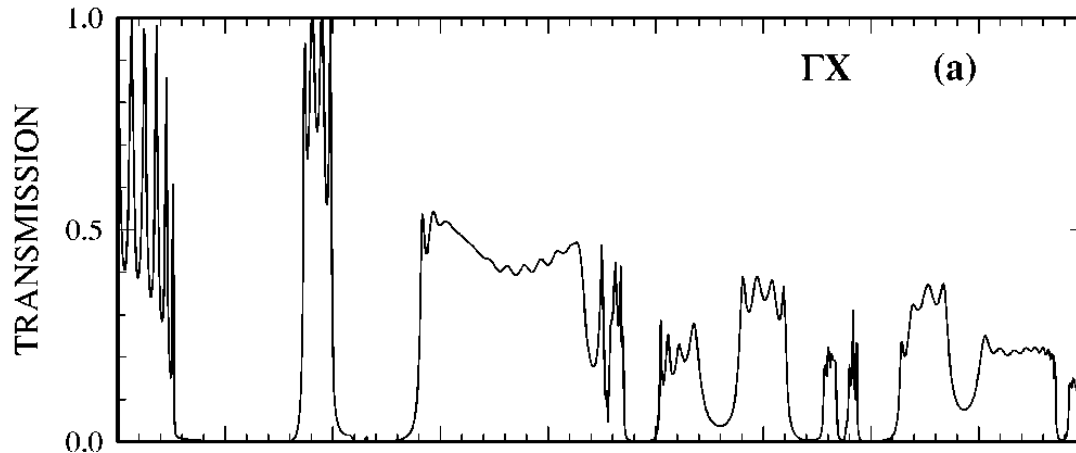
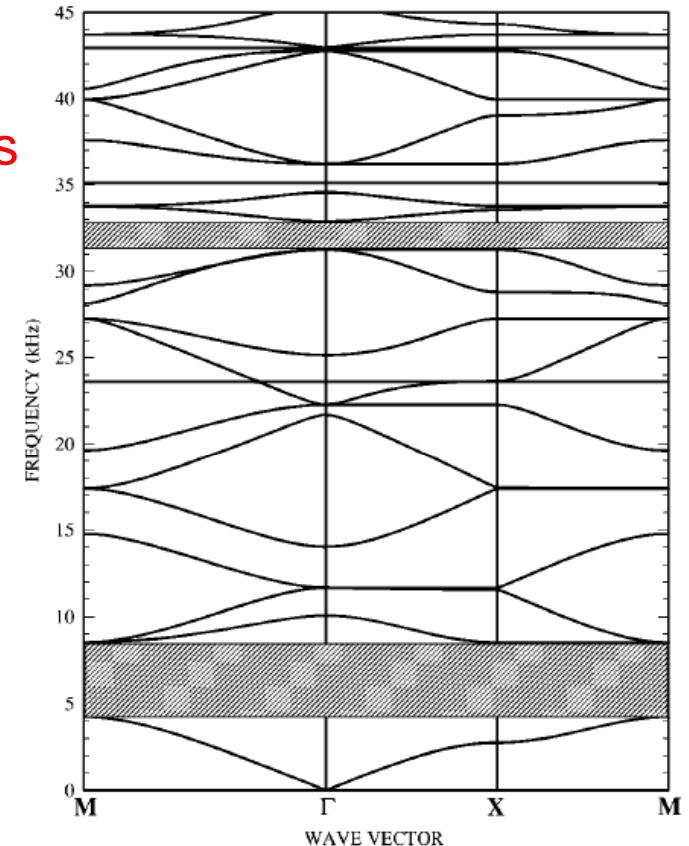


Early Work in Phononics

Bandgap Structures:



2-D structure with copper rods
 • Bragg scattering

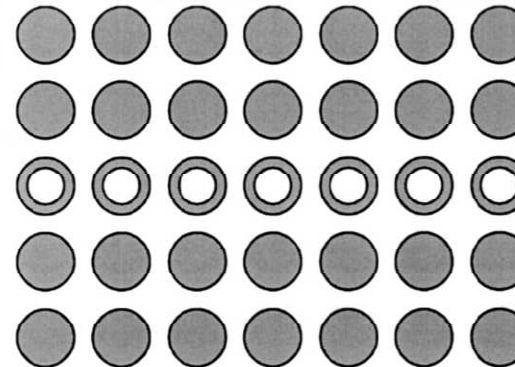


- Ranges of certain frequencies cannot be transmitted.

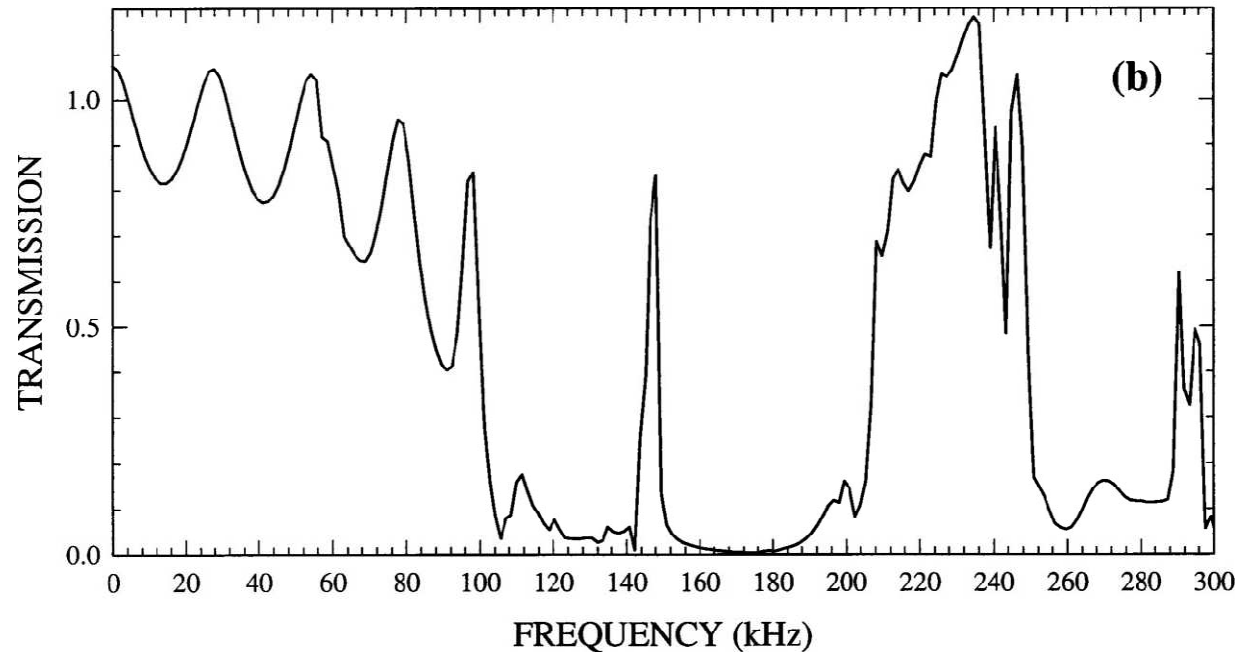
Early Work in Phononics

Waveguide Structures:

2-D structure with hollow steel rods



(a)



(b)

Phononic Metamaterials: Current Strategy

Novel utilization of real/k-space functionality of metamaterials

- refractive properties
- spatial scaling: macro to nano functionalities
- using Bragg scattering

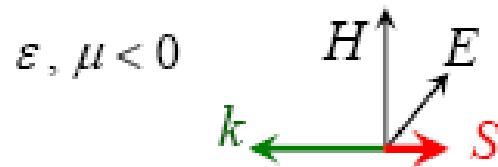
To ensure real space control of phononic propagation over a broad spectral range (acoustic to atomic-vibrations)

- **Superlensing: Acoustic imaging**
- **Acoustic collimation**
- **Thermal interface materials (TIM): Ballistic phonon transport**
- **Thermoelectrics (TE)**

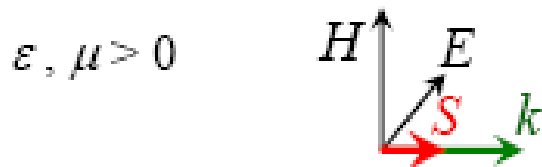
Negative refraction-Left-handed materials

Left-Handed Materials (LHMs) were considered by Veselago¹

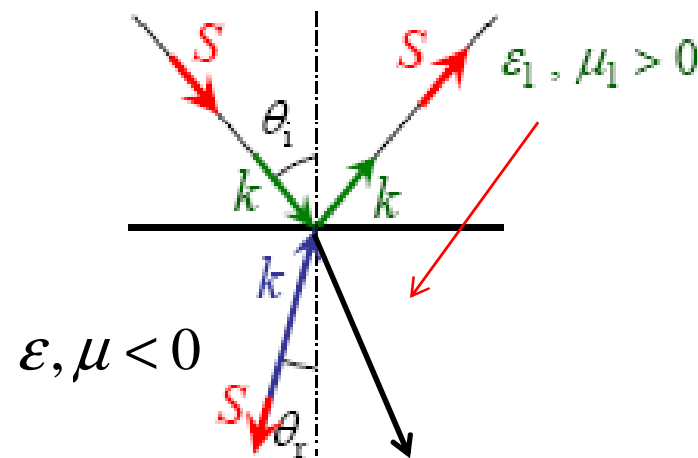
Left-Handed materials: k and S
are in opposite directions



Right-Handed materials: k and S
are in the same direction



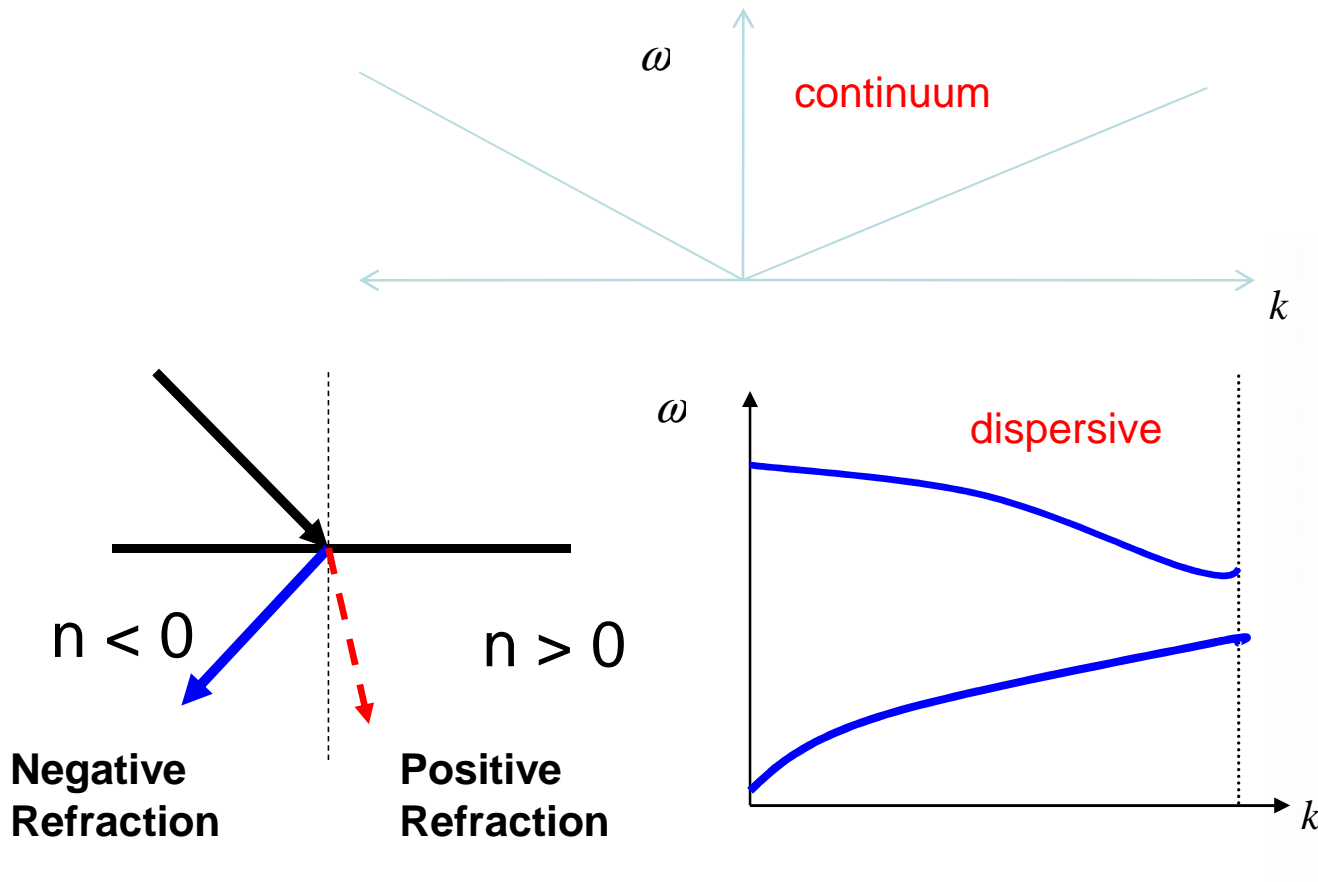
Veselago¹ also predicted the unusual
phenomenon of negative refraction:



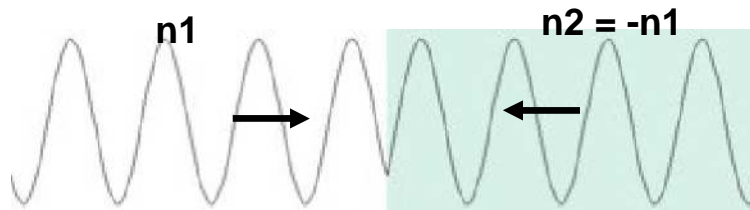
¹ V. G. Veselago, Sov. Phys. Usp. 92, 517 (1964)

Negative refraction in phononic metamaterials:

1. Bragg scattering (phononic crystals)
2. Locally resonant materials ($\rho < 0, C_{ij} < 0$)

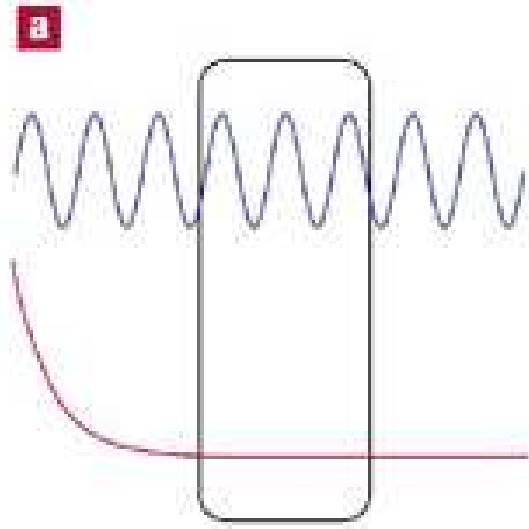


Bands of **negative slope** represent frequencies at which **negative refraction** will occur.



***However: Energy still flows to the right.**

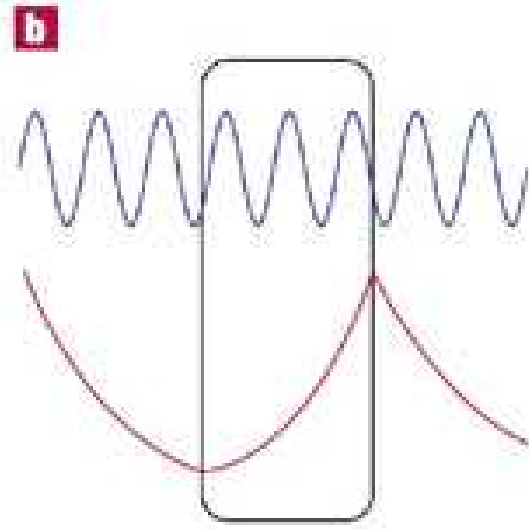
Phononic Crystal Super Lens



Conventional Lens

(Loss of Evanescent Component)

Diffraction limit = $\lambda/2$

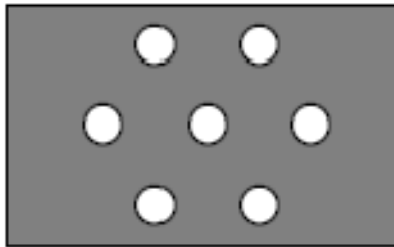
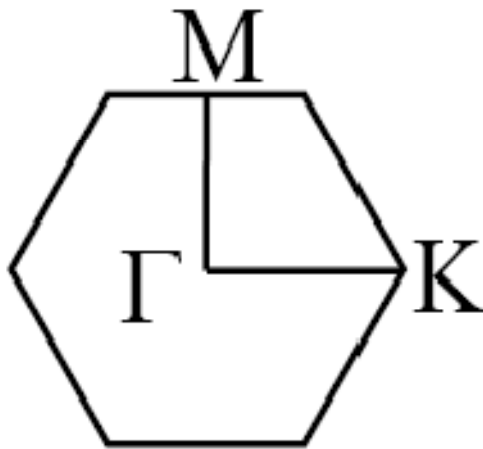


Near-Field Super Lens

(Amplification of Evanescent Component)

Solid-fluid phononic crystal with negative refraction

Steel cylindrical inclusions in fluids (methanol)



Inter-cylinder spacing (a)=1.27mm,
 Cylinder diameter=1.02mm

Steel:

Density= 7780kg/m³

Longitudinal speed of sound=5825m/s

Transverse speed of sound=3227m/s

Methanol:

Density=790kg/m³

Speed of sound=1138m/s

PRL 102, 154301 (2009)

PHYSICAL REVIEW LETTERS

week ending
 17 APRIL 2009

Experimental and Theoretical Evidence for Subwavelength Imaging in Phononic Crystals

A. Sukhovich,¹ B. Merheb,² K. Muralidharan,² J. O. Vasseur,³ Y. Pennec,³ P. A. Deymier,² and J. H. Page¹

Methanol/Steel phononic crystal

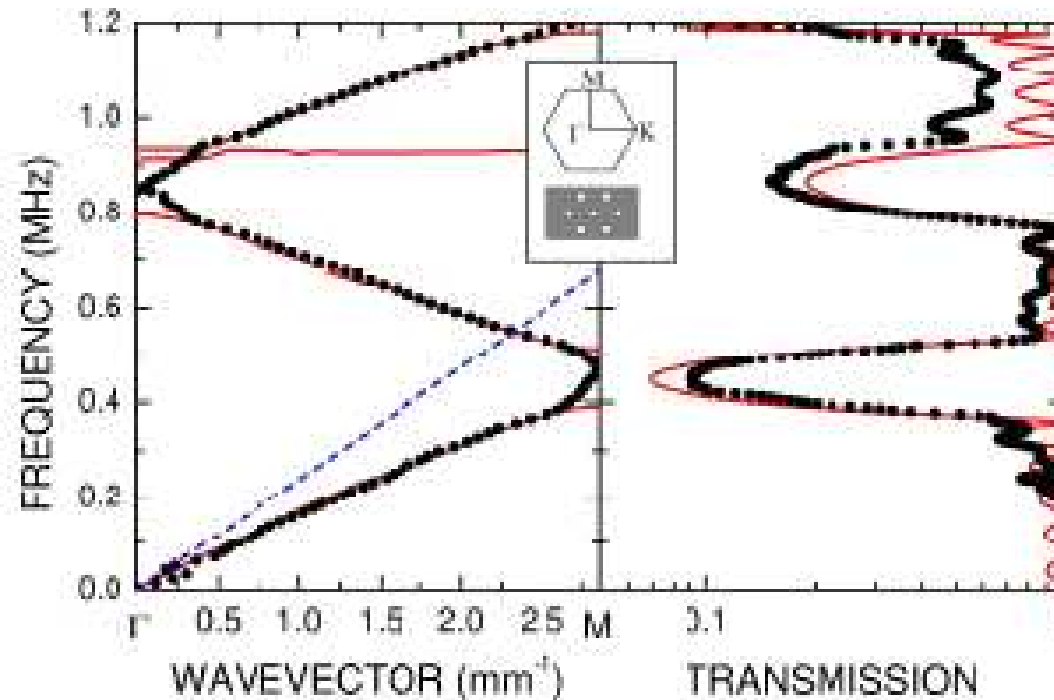
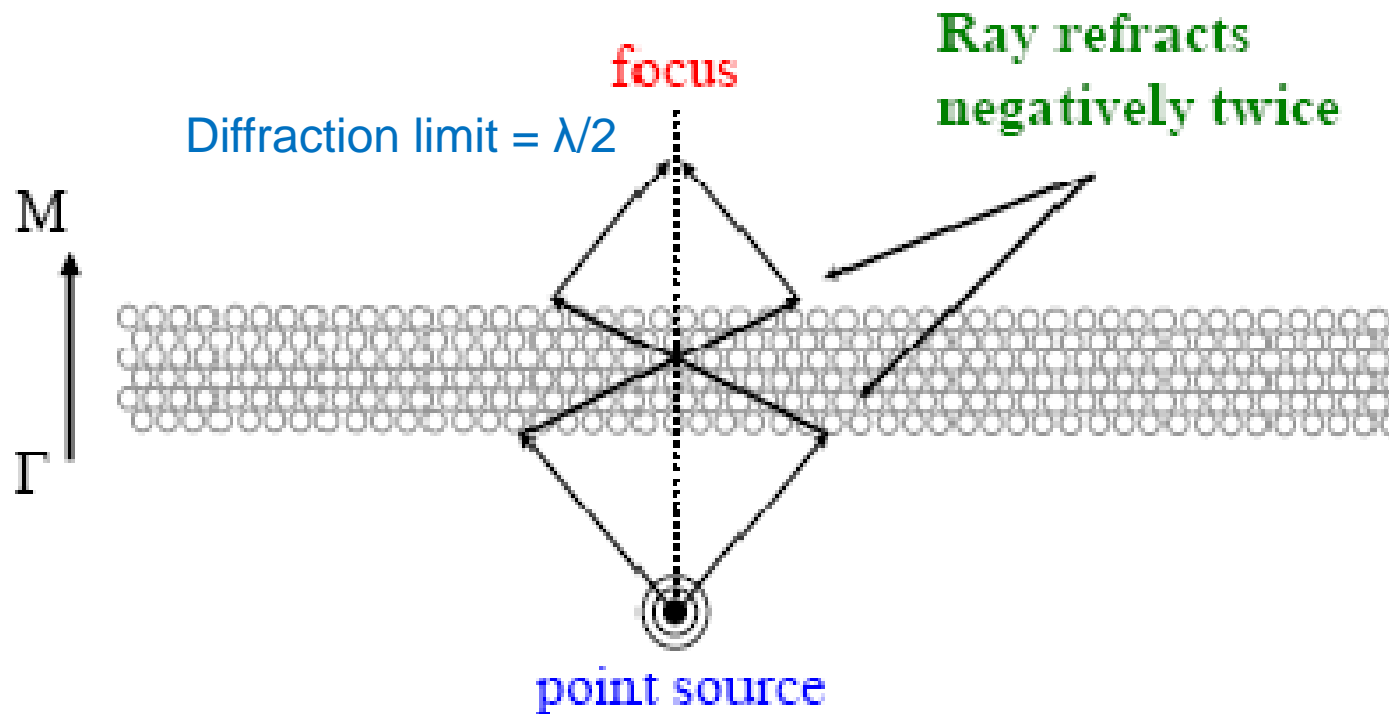


FIG. 2: Band structure of the methanol-steel phononic crystal in the ΓM direction of the first Brillouin zone (left panel) and transmission coefficient for a 8-layer crystal along the same direction (right panel): symbols, experimental data; solid red lines, FDTD calculation; dashed blue line, homogeneous water. The inset illustrates the phononic crystal structure and the associated first Brillouin zone.

Sound focusing in phononic crystal



FDTD method

- Discretize space $dx=dy=2 \times 10^{-5} \text{m}$
- X axis parallel to flat lens
- Z axis perpendicular to flat lens
- Absorbing Boundary Conditions in all directions

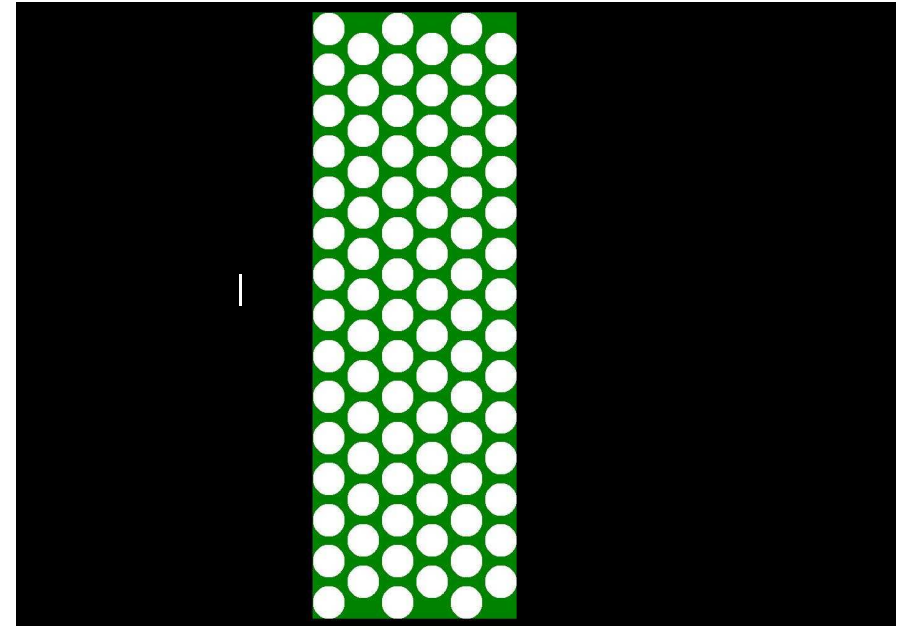
Line source as a model of the pinducer:
along a line 0.55mm long // x axis:

$$u_x = u_x + \cos(\omega t)$$

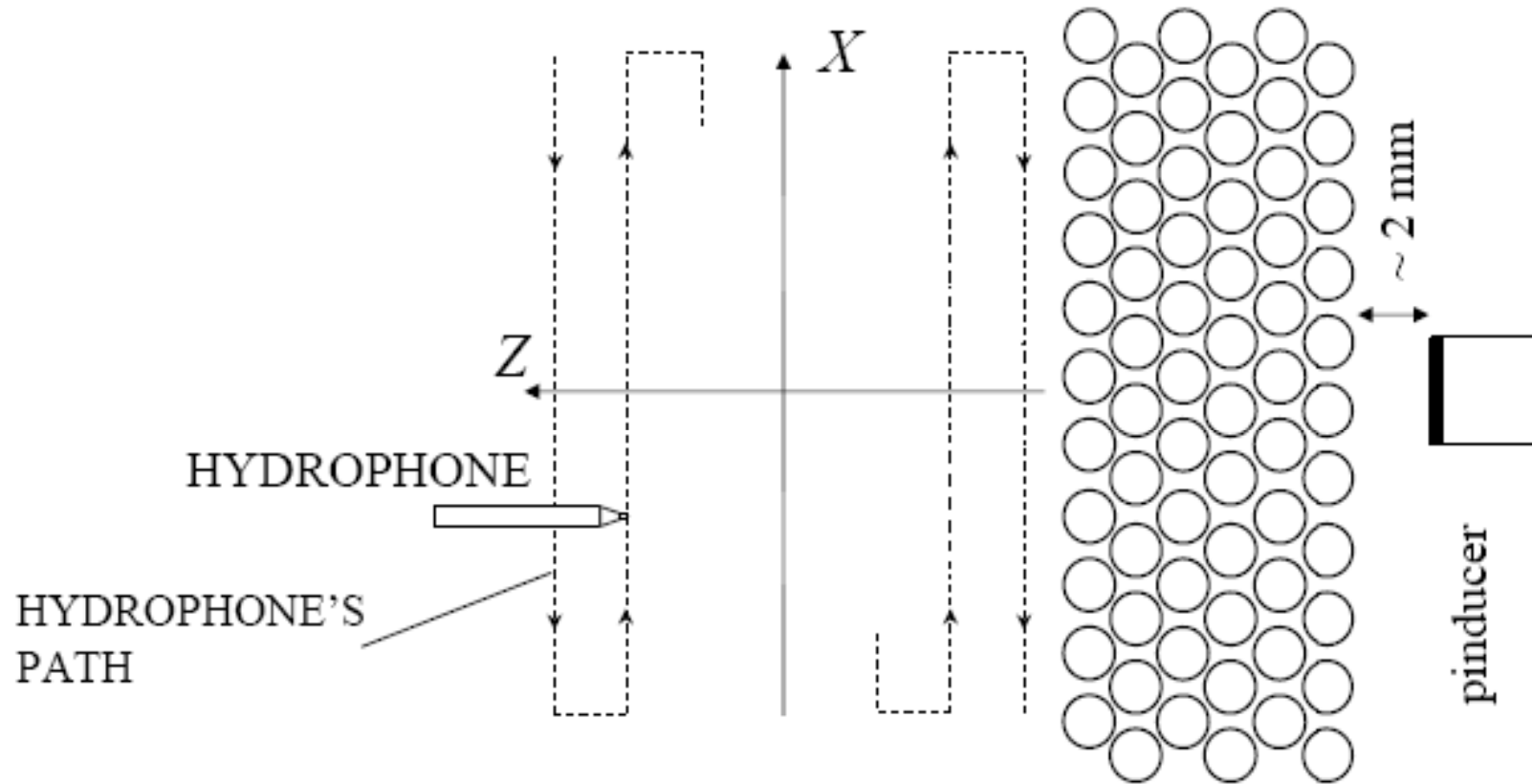
$$u_z = u_z + \cos(\omega t)$$

Lateral length = $60a$

Distance of source to lens = 1.6 or 0.1mm



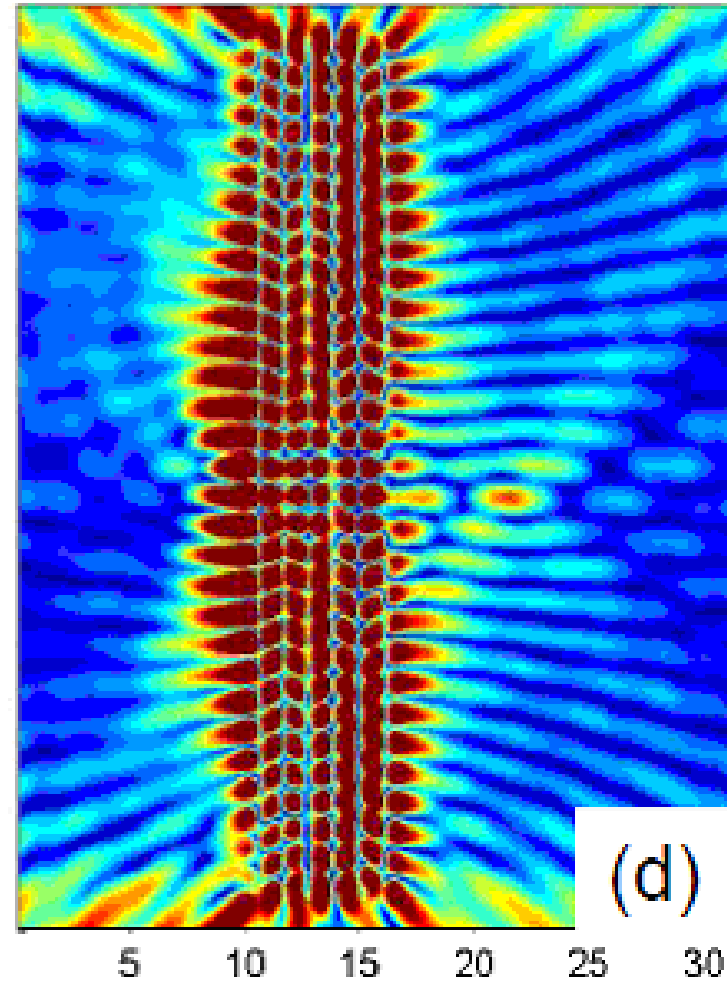
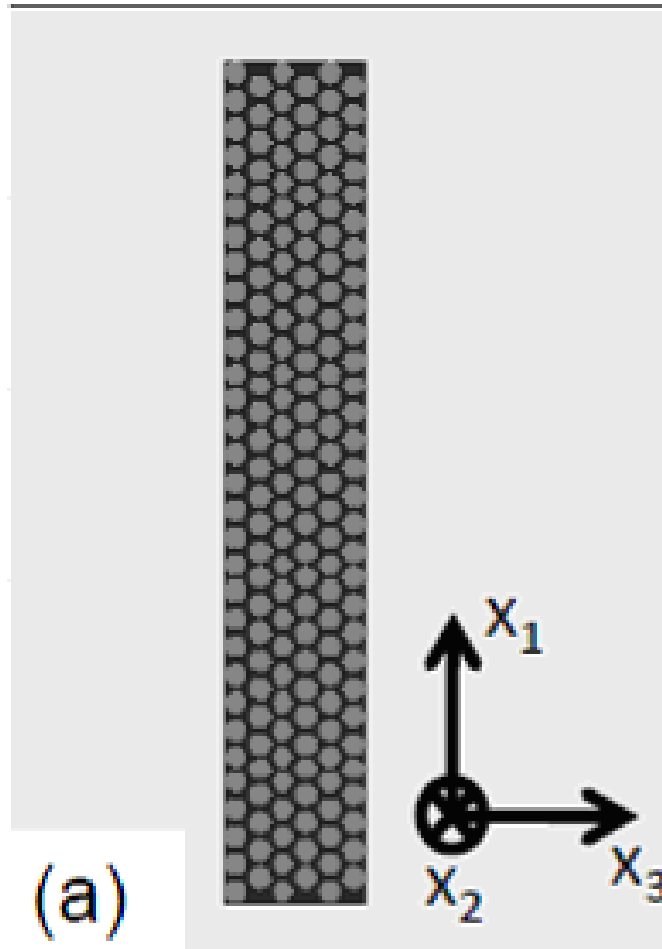
Experimental measurements



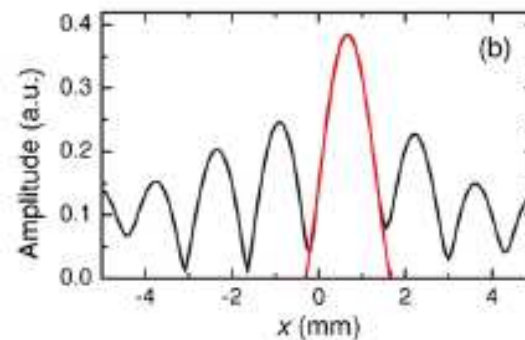
Lens immersed in water



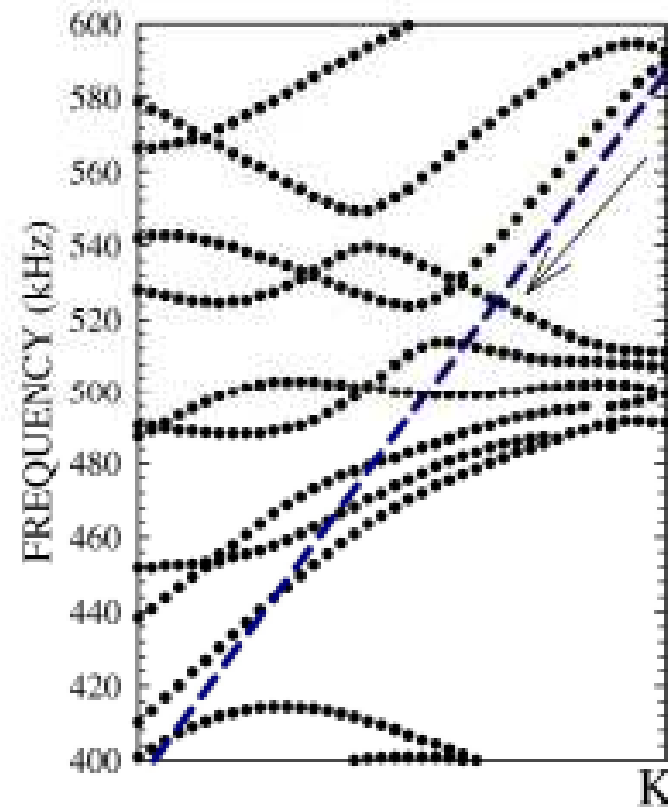
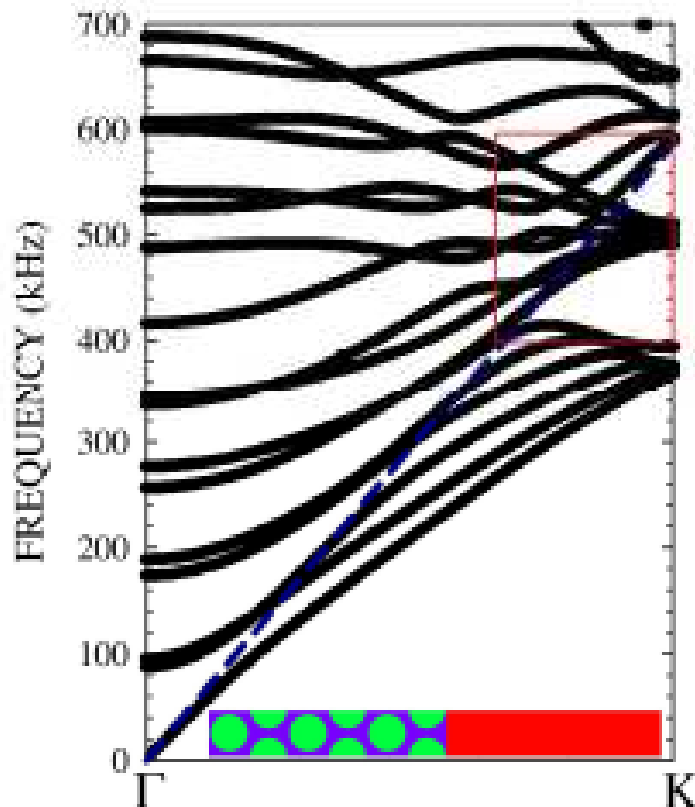
Phononic Crystal Super Lens



0.35 Lambda

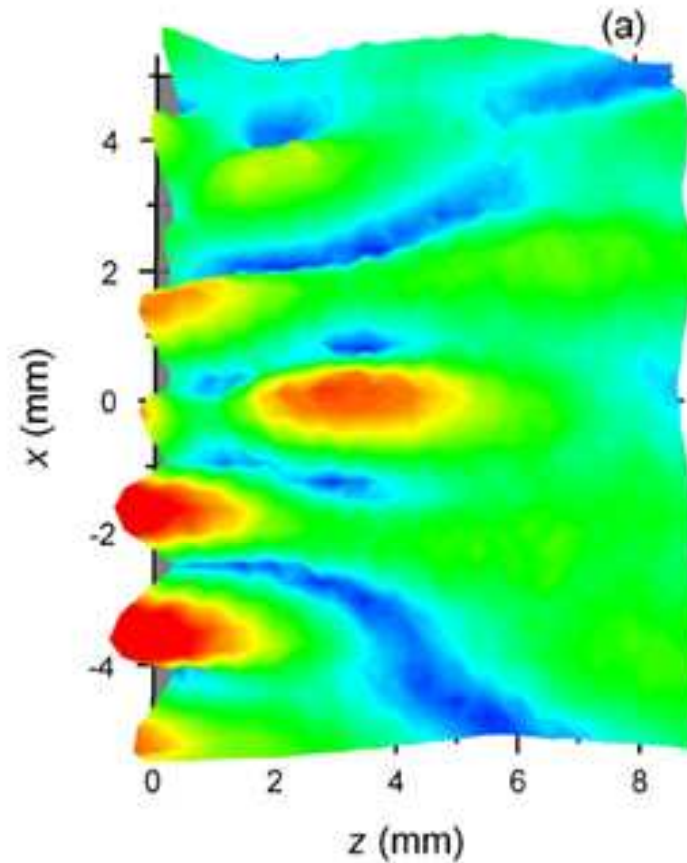


Band Structure Calculations

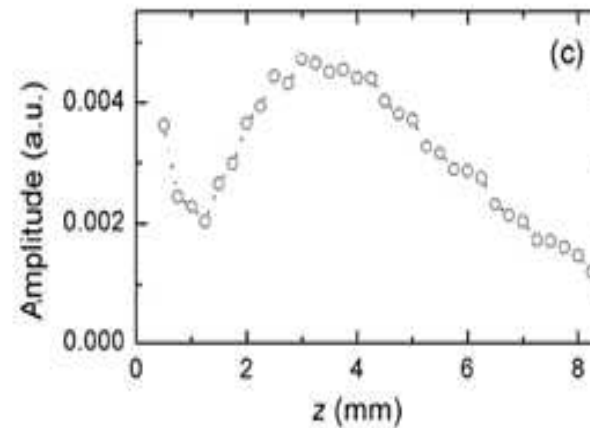
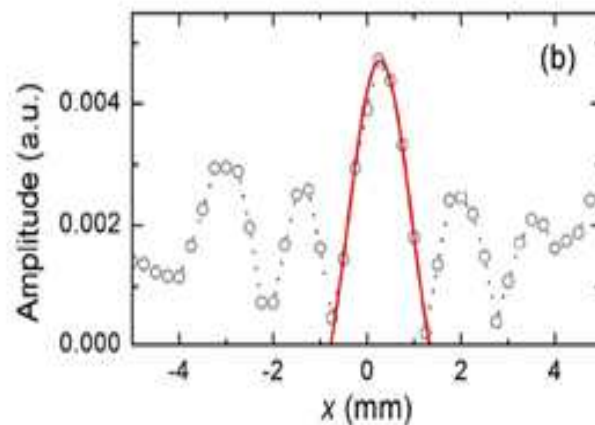


- Evanescent components excite the bound modes of the crystal, leading to its amplification.

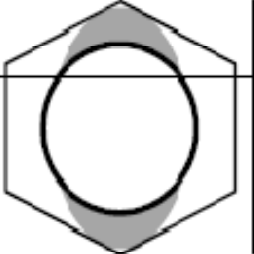
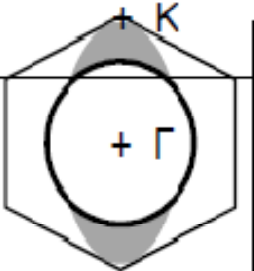
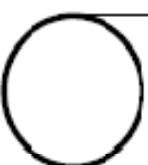
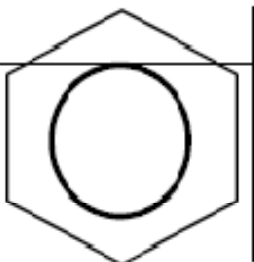
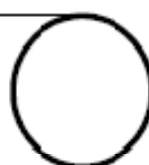
Experimental Validation

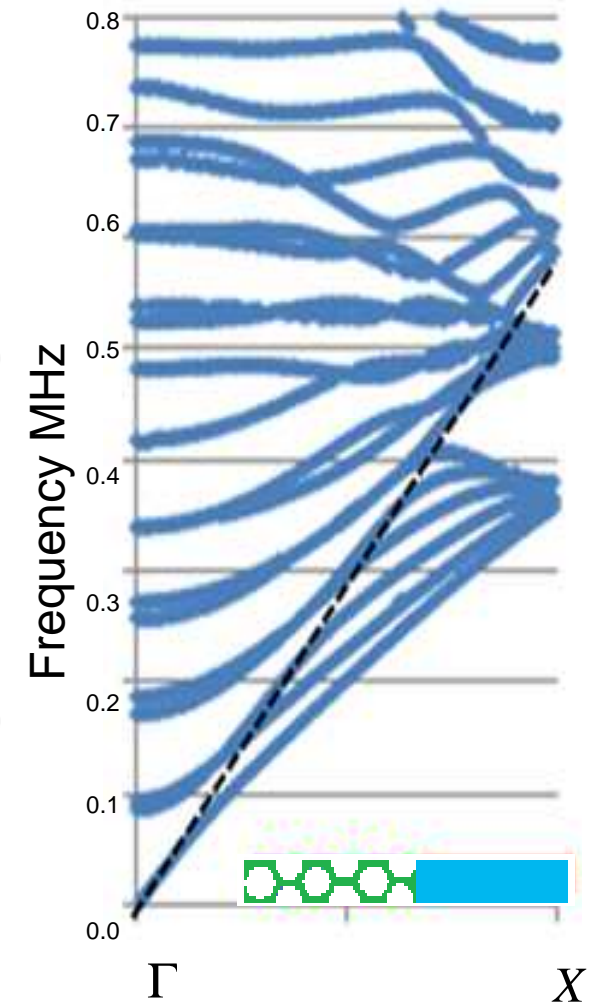


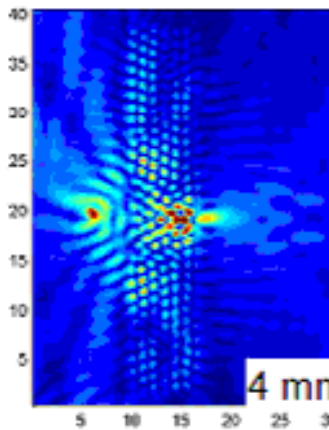
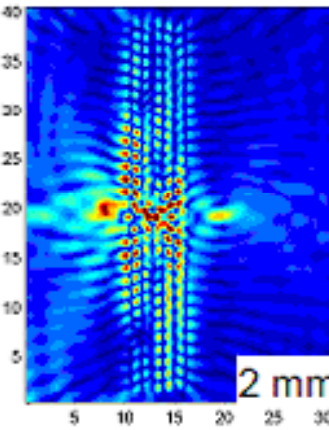
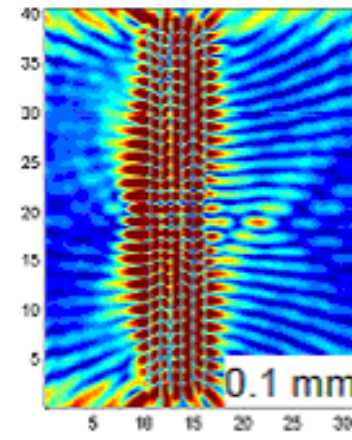
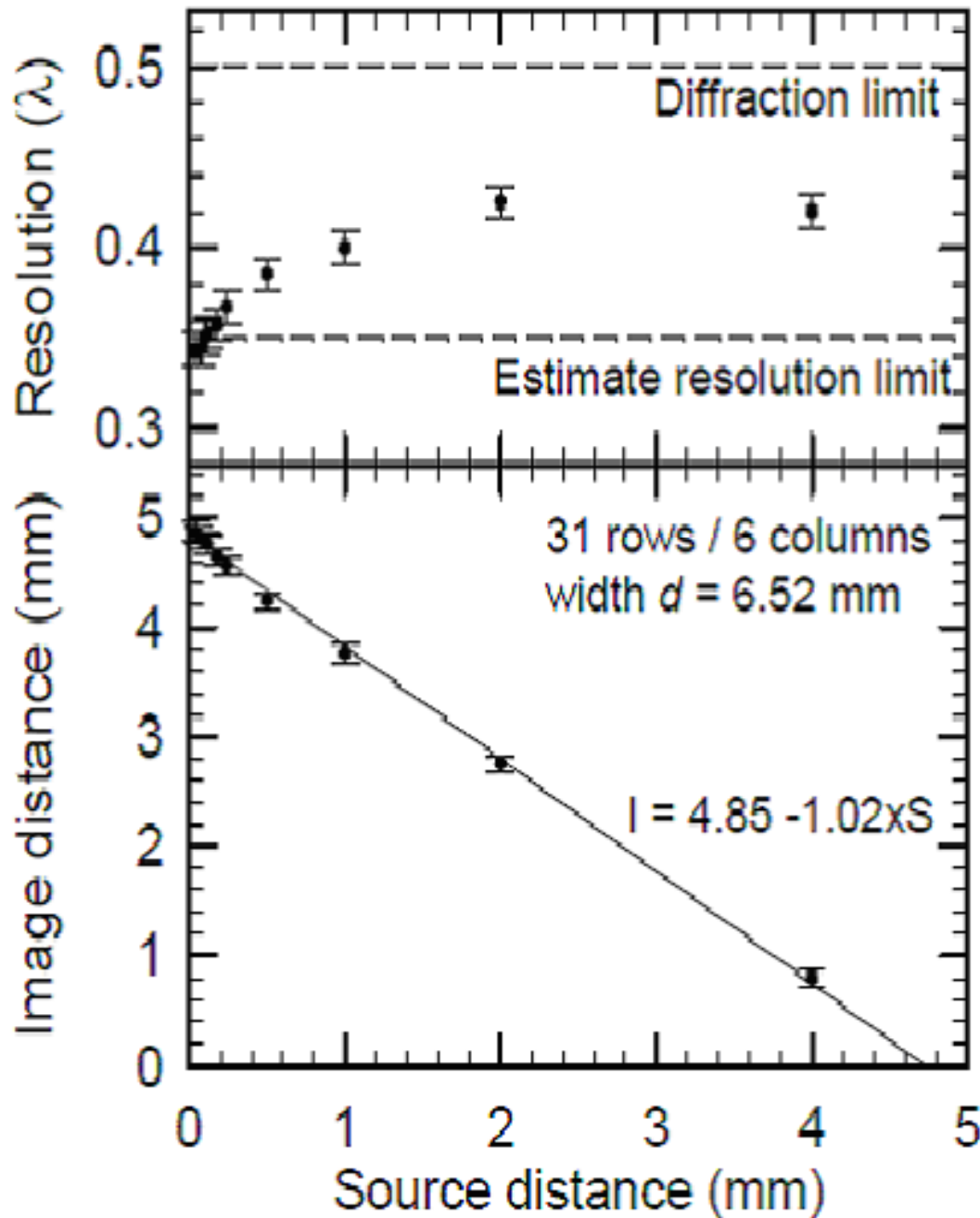
Resolution = 0.37λ



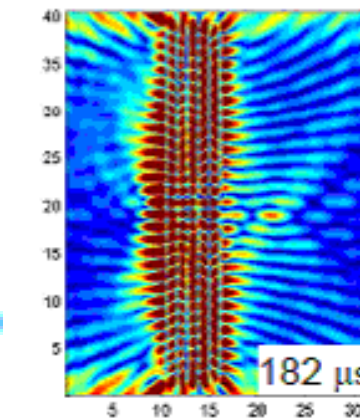
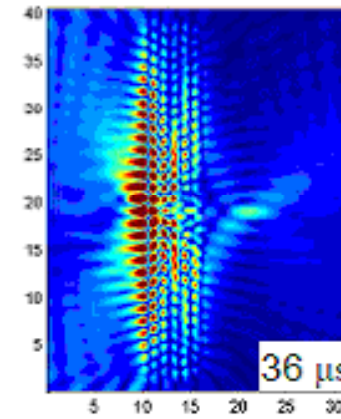
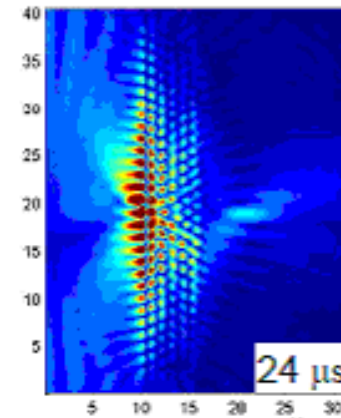
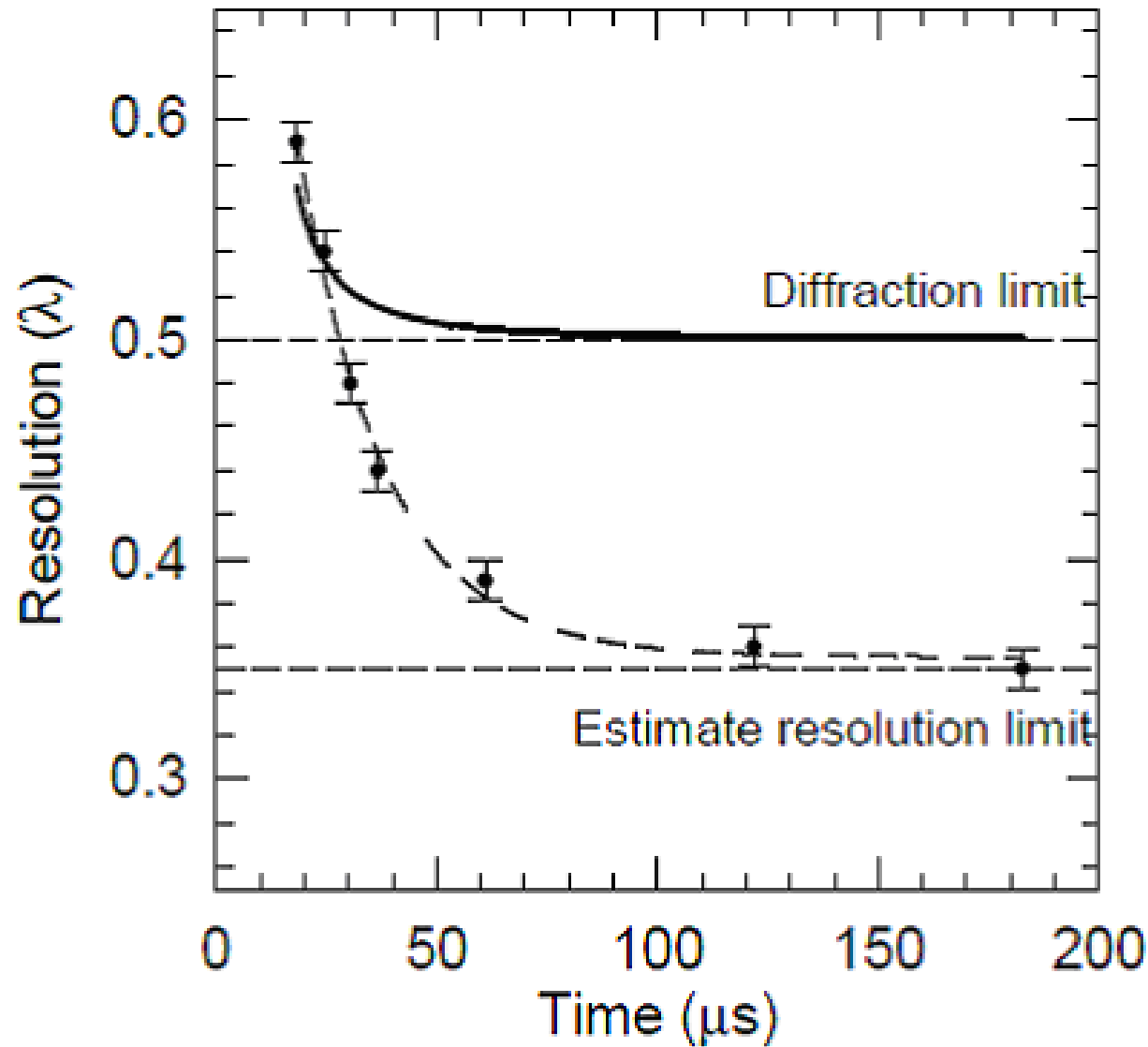
Operation Frequency

Water	PC	Water	Freq. (kHz)	Resol.	Position (mm)
			515	0.34λ	2.56
			530	0.35λ	4.80
			545	0.47λ	5.84



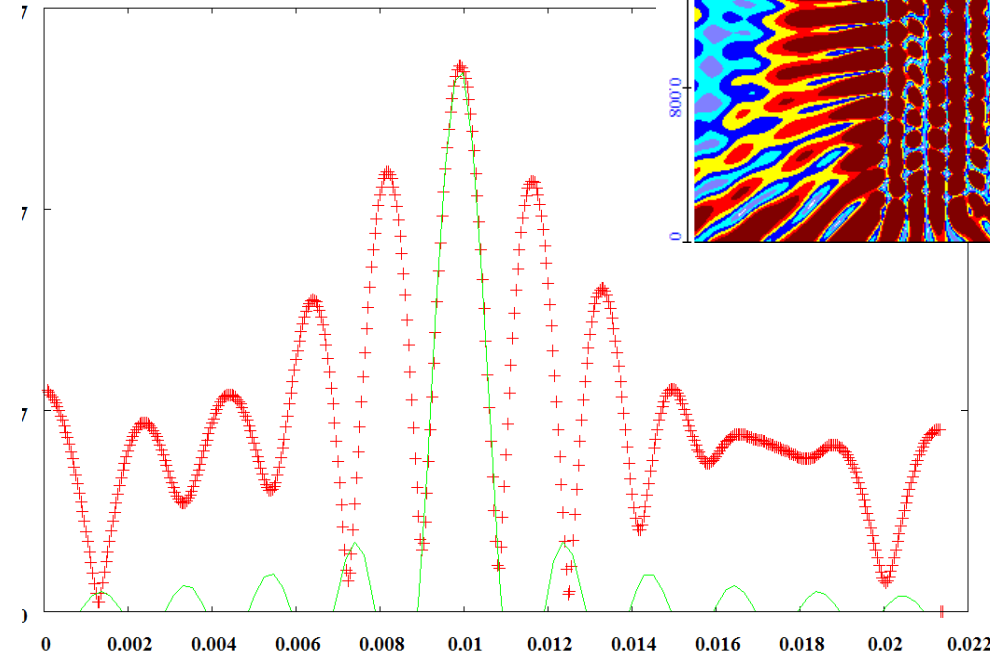
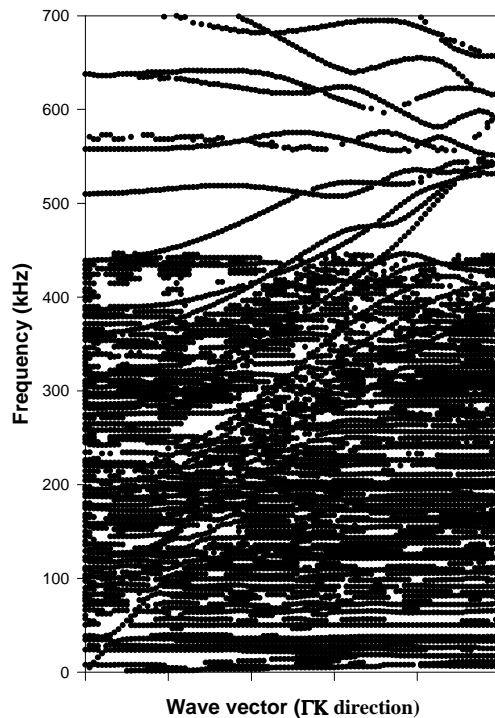
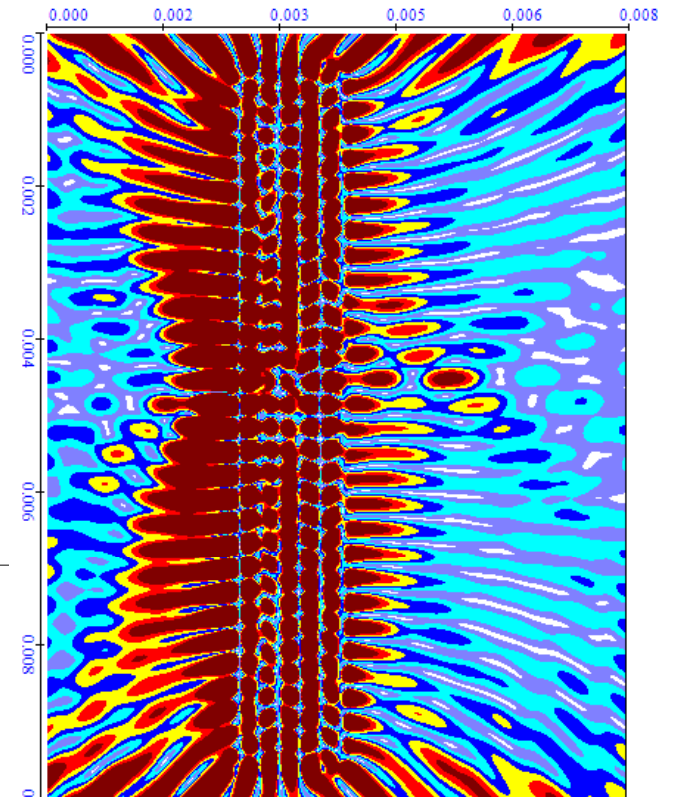


Time dependent Resolution



Rubber/Steel/Water Phononic Crystal

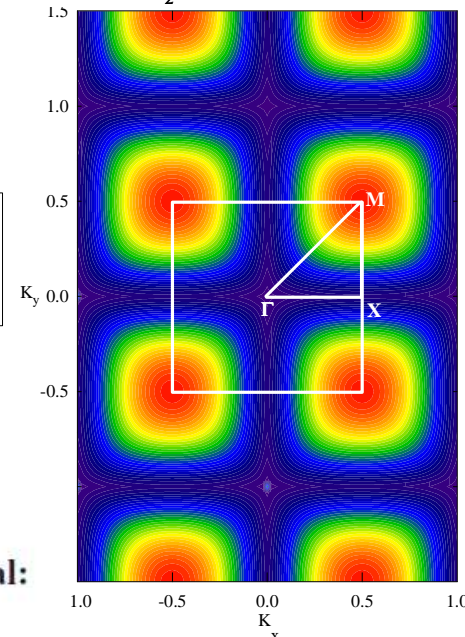
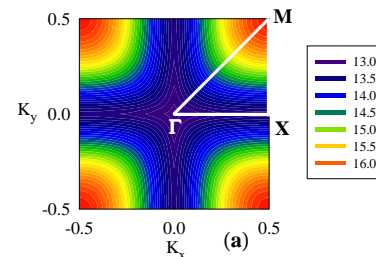
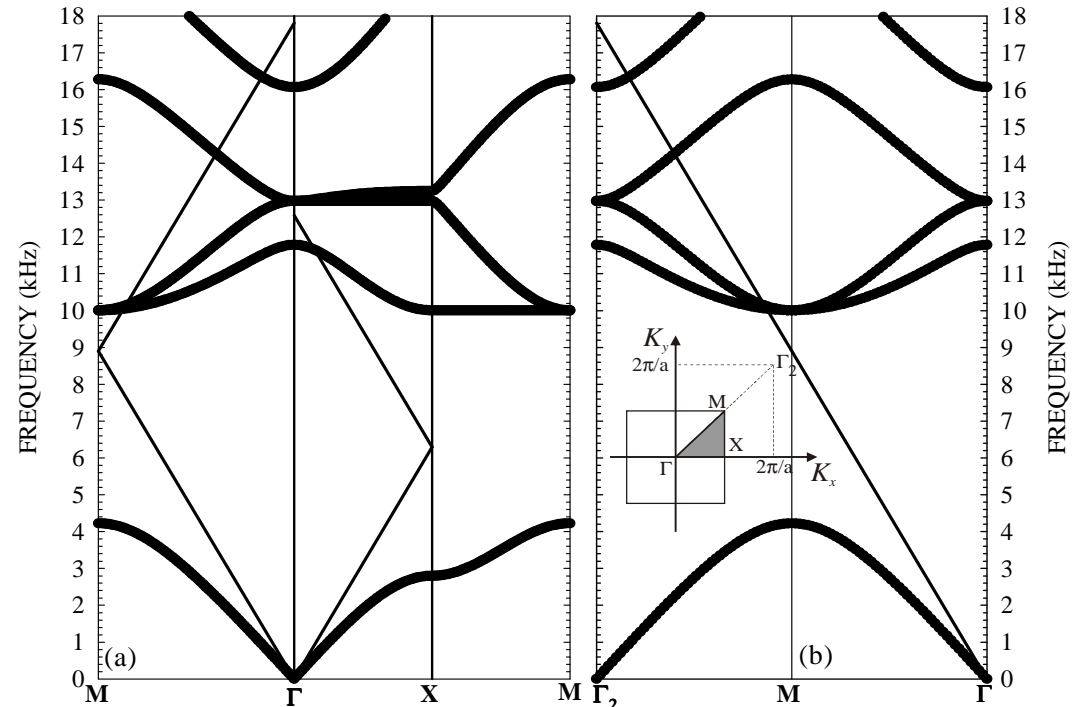
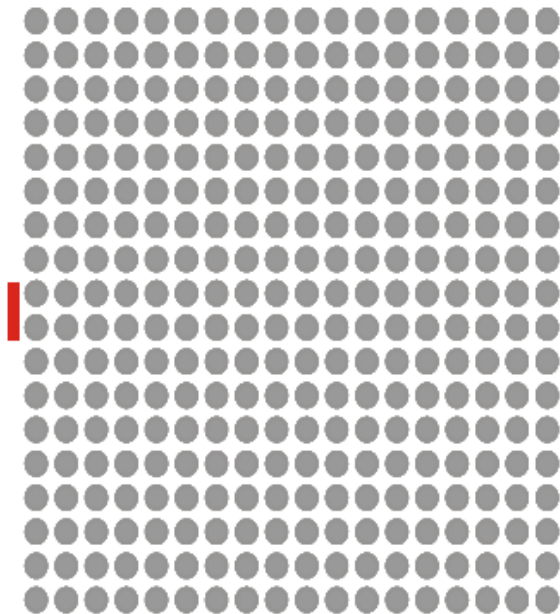
	$\rho(kg/m^3)$	$C_l(m/s)$	$C_t(m/s)$
Rubber	1000	1200	20
Water	1000	1490	0
Steel	7780	5825	3227



Resolution = 0.35λ

PVC-Air crystal

- PVC cylindrical inclusions (r=12.9mm)
- Air Matrix
- Square lattice (a = 27mm)



PHYSICAL REVIEW B 79, 214305 (2009)

Positive, negative, zero refraction, and beam splitting in a solid/air phononic crystal:
Theoretical and experimental study

Frequency contours: 4th band

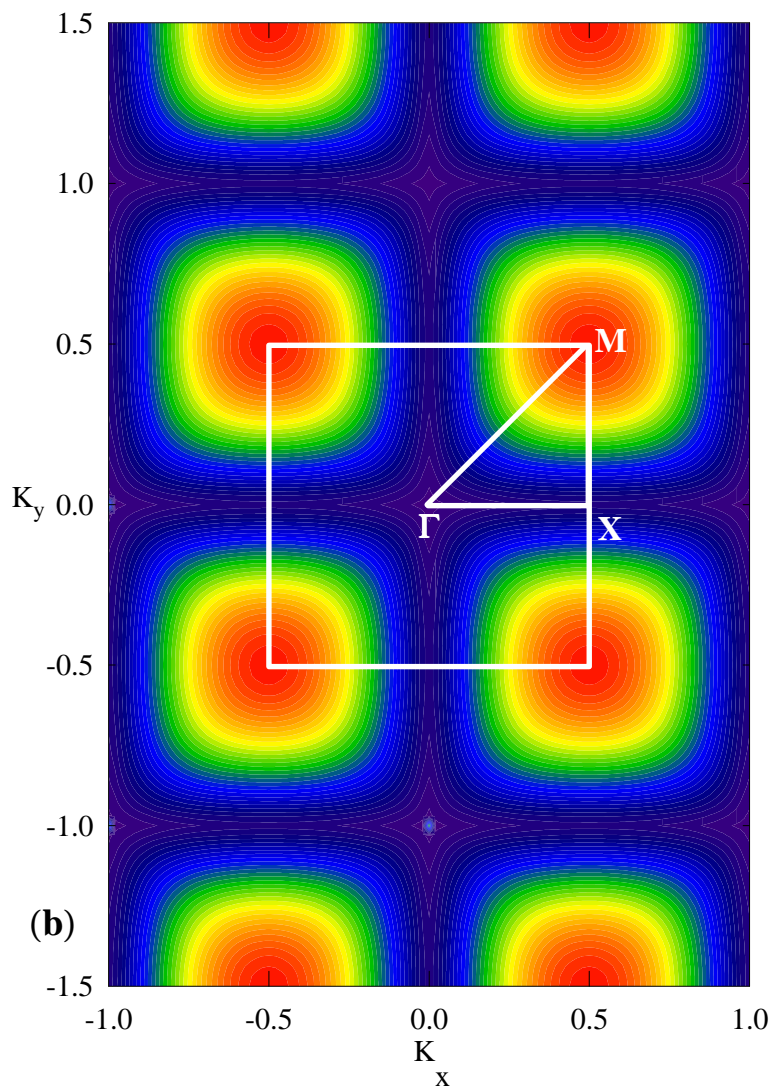
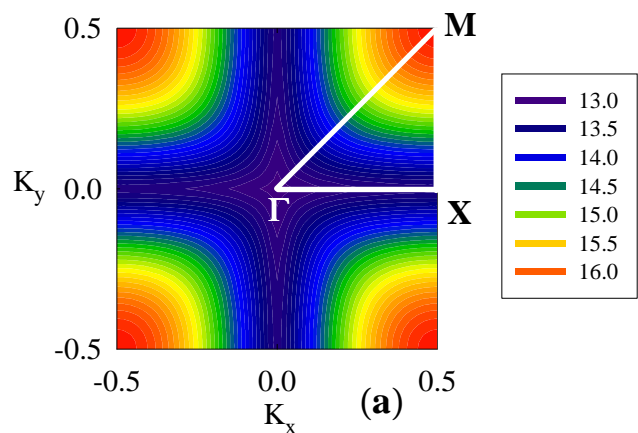
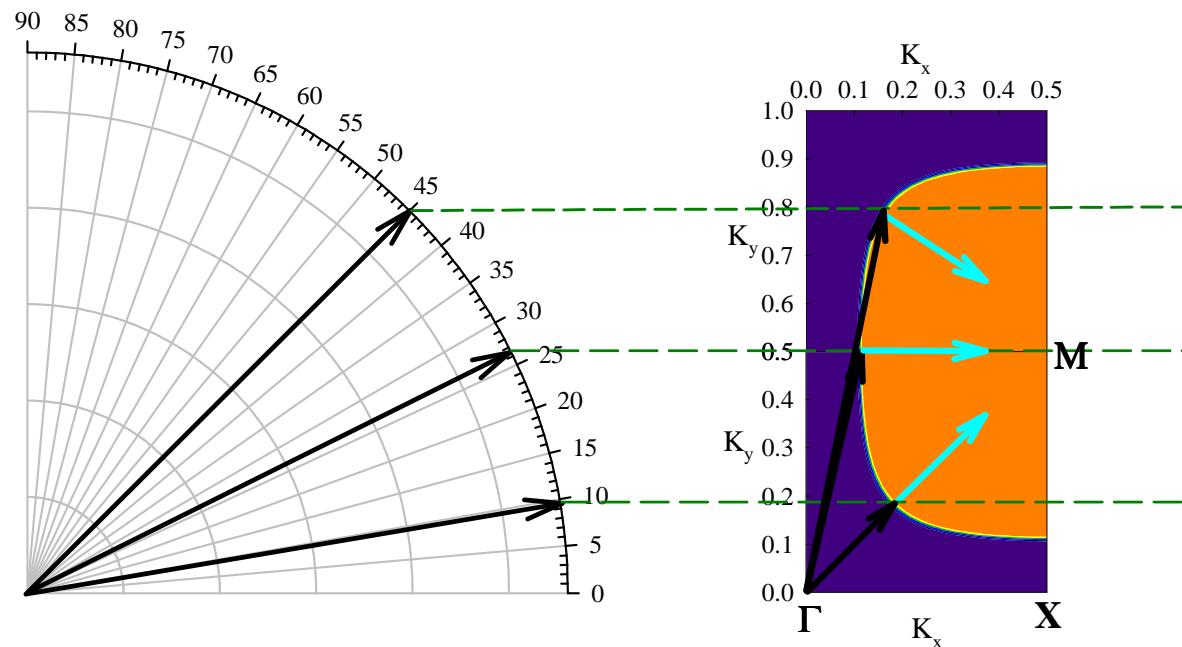
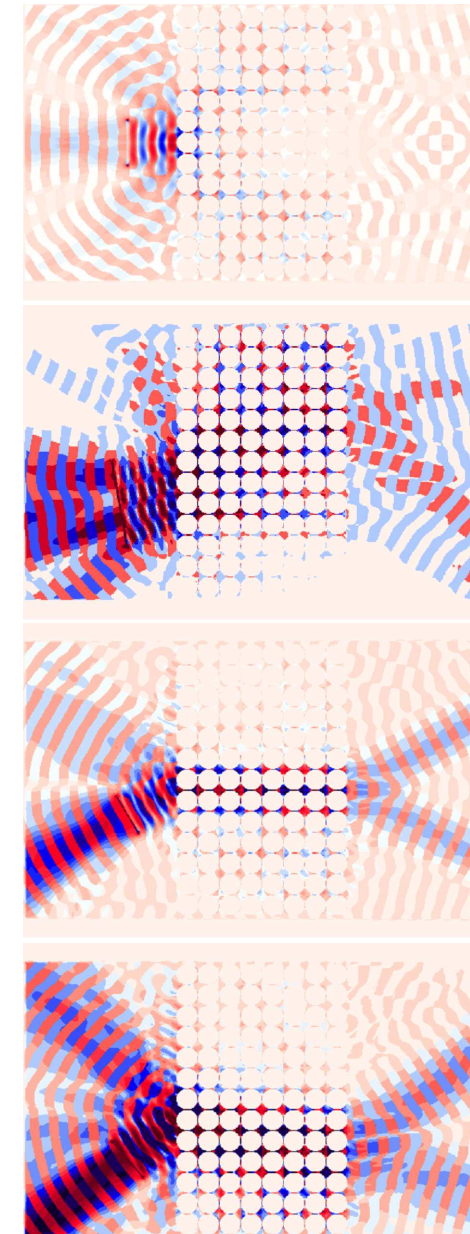


Figure : Equifrequency surface corresponding to the fourth band in the first Brillouin zone (a) and in an extended zone scheme (b). The EFS of the PC calculated inside the first Brillouin zone (a) has been repeated by a large number of translations of the reciprocal vectors. One notes that in the extended zone scheme, the EFS are centered on the M point and are of square shape except at their corners.

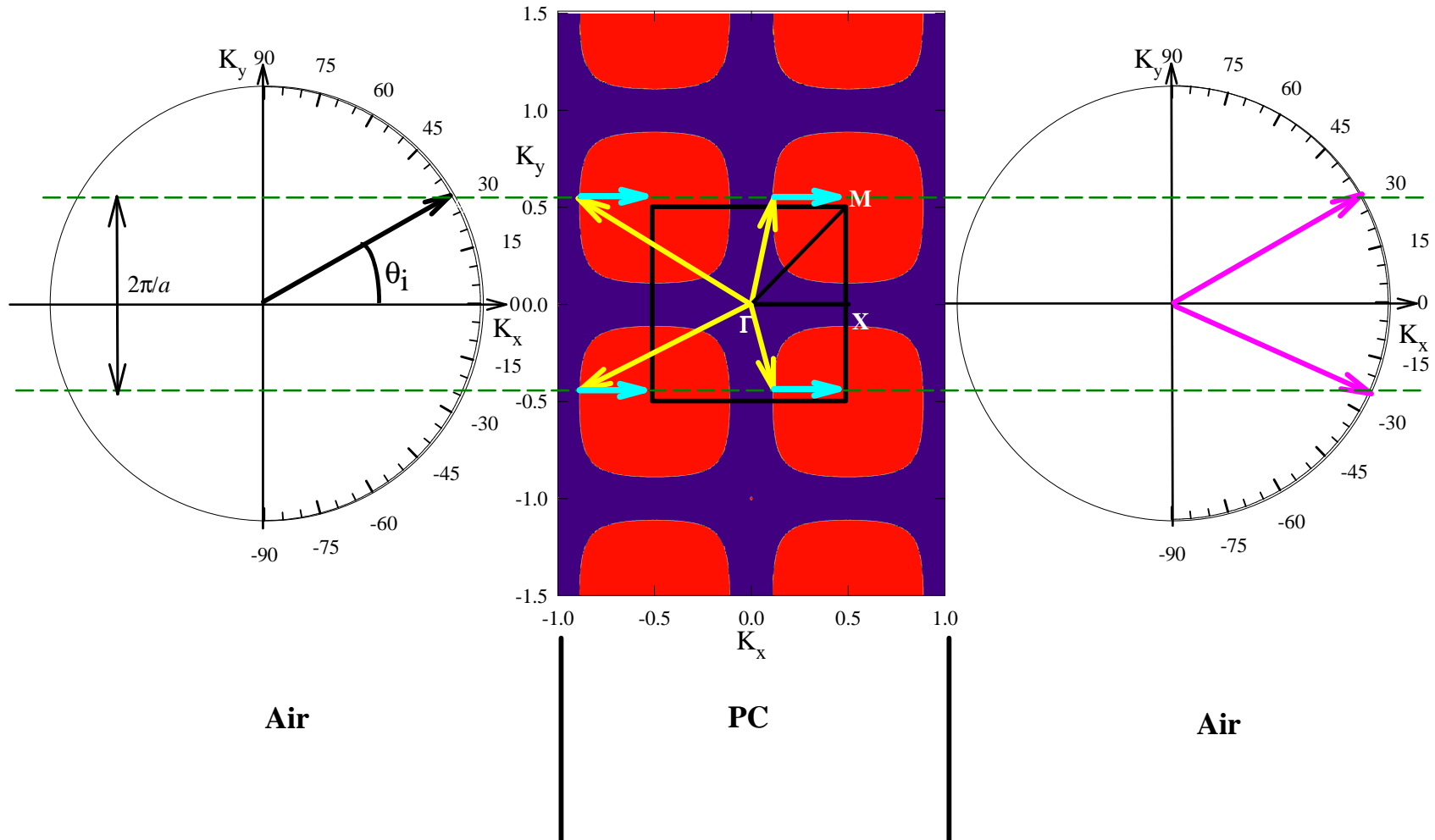
Positive, Negative, and Zero-angle Refraction



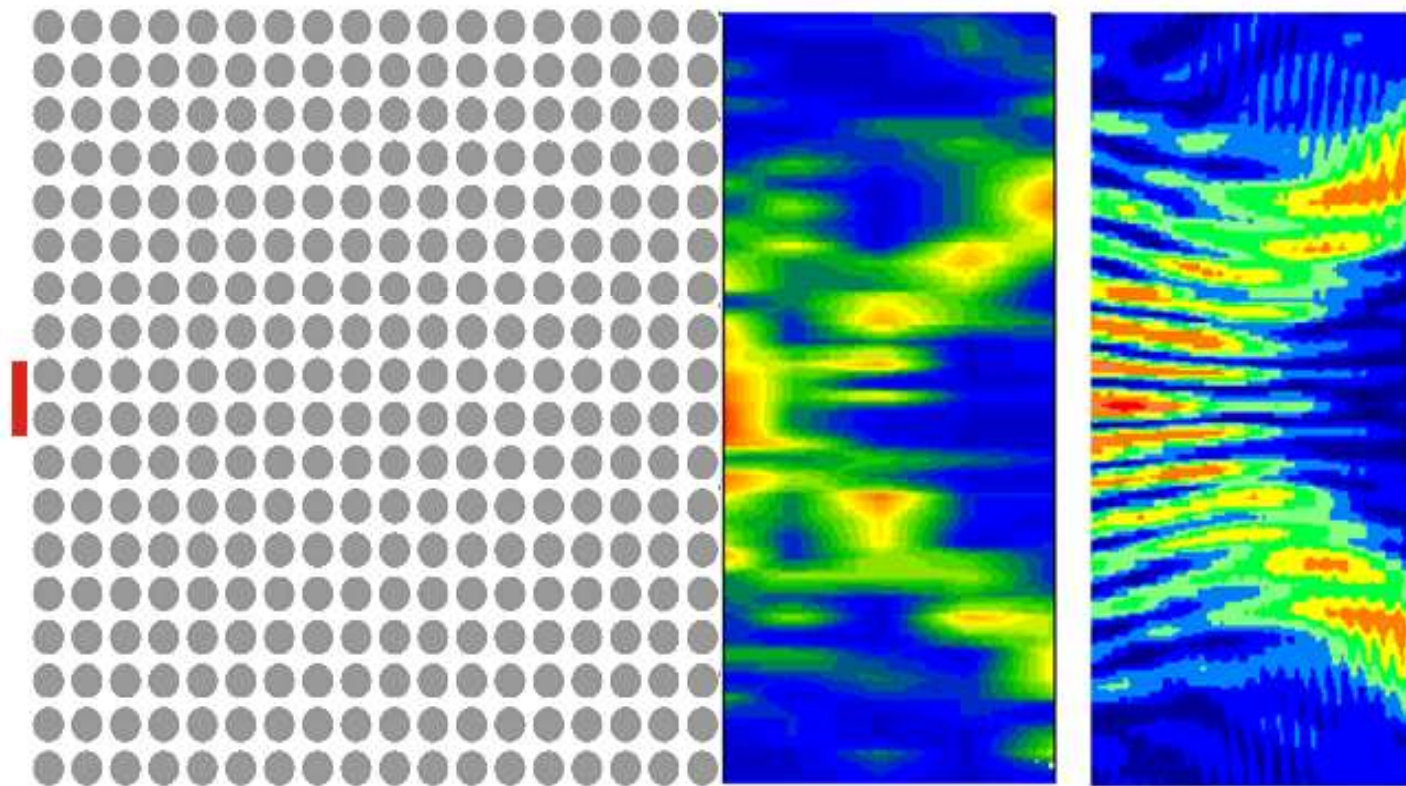
✓ Collimation of waves



Beam Splitting



Validation of Beam Splitting

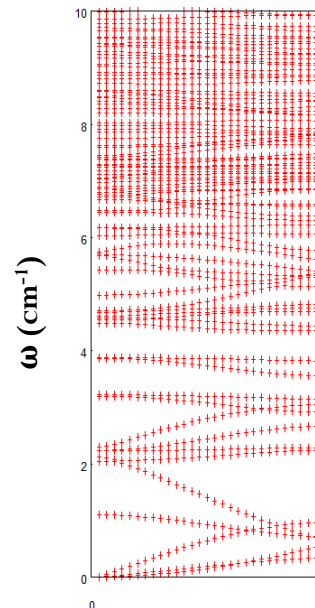
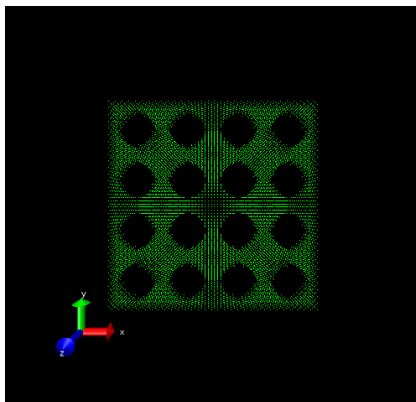


Experiment

Simulation

Thermal Management

- Heat harvesting offers tremendous potential for energy management during chip operation
- **Thermoelectrics (TE)**
- Thermal screening is critical to ensure safety and security in many areas (e.g. thermal barrier films)
- Heat dissipation methods: reduce hot spots in chips
- **Thermal Interface Materials (TIM)**



Thermal Conductivity

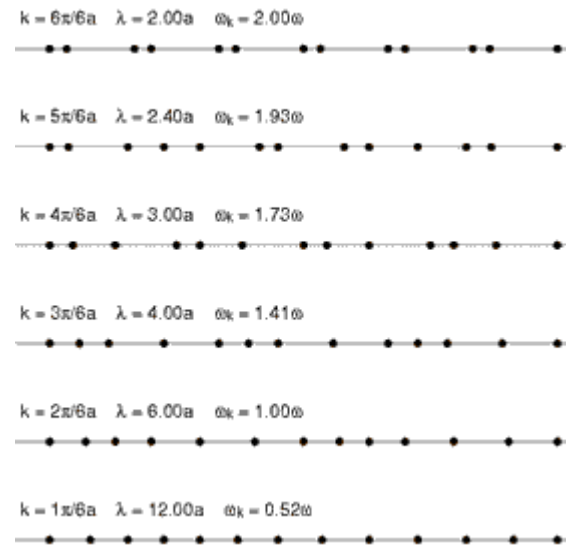
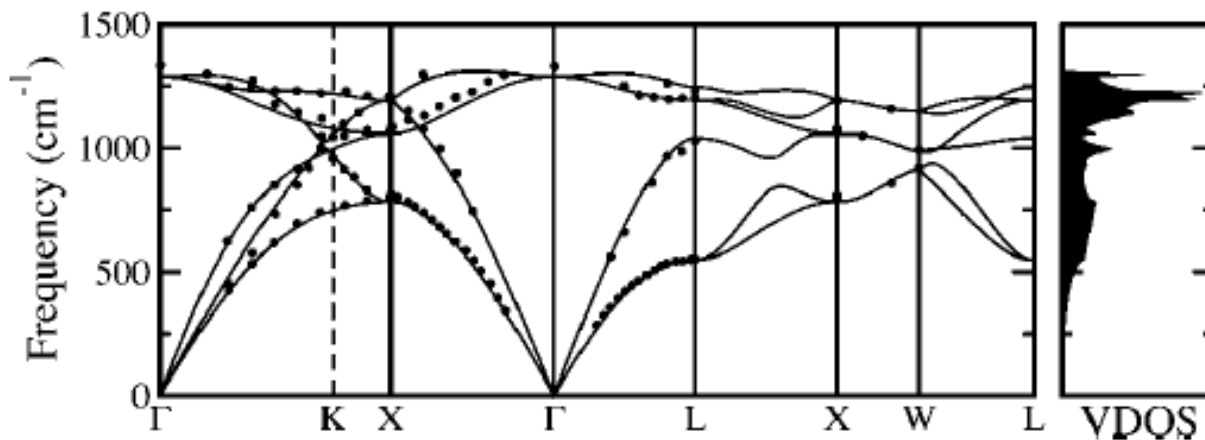
Fourier law defines thermal conductivity
Coefficient heat flux / thermal gradient

$$J = -\bar{k} \cdot \vec{\nabla} T$$

↓
tensor

Most heat is carried by:

- electrons → Main heat carriers in metals
- phonons → In the low frequency regime phonons are equivalent to sound waves
→ Only heat carriers in insulators



$$\bar{k} = \sum_{\omega} \sum_{\vec{q}} c(\omega, q) \vec{V}_g(\omega, q) \vec{V}_g(\omega, q) \tau(\omega, q)$$

↓ heat capacity ↓ group velocity ↓ phonon mean life-time

Thermoelectric materials for energy harvesting

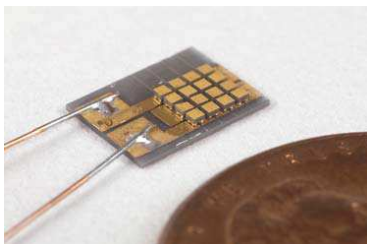
The ability to harvest the heat produced and recycle it back as DC electric power is an invaluable method of reducing power consumption during semiconductor chip operation

THERMOELECTRICS (TE):

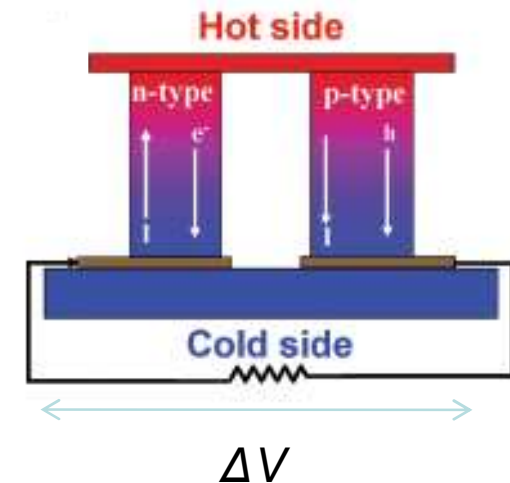
- Transformative technology for energy conversion (heat to electricity)
- Based on Seebeck effect: A temperature difference (ΔT) across a material gives rise to a corresponding electrochemical potential (ΔV); the Seebeck coefficient (S) equals ΔV generated per unit temperature gradient.
- Typical TE devices consist of alternating n-type and p-type materials, such that

$$\Delta V = (S_p - S_n) \times \Delta T$$

semiconductors have intrinsically higher Seebeck coefficients (are 10^3 greater than metals)

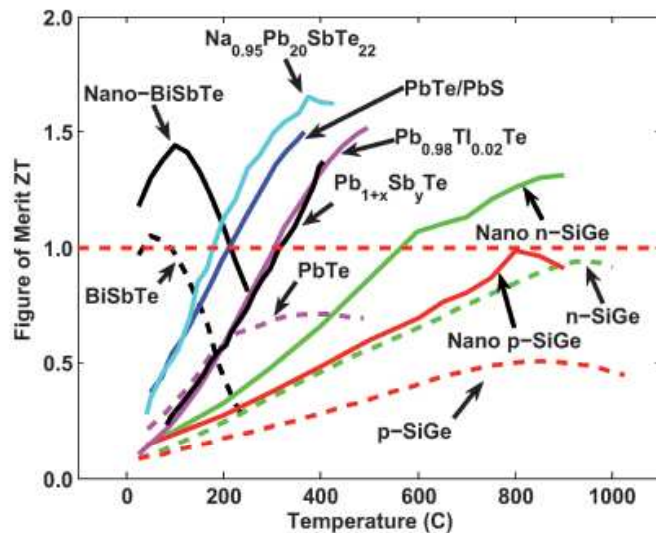


Venkatasubramanian et al.,
 IEEE, (2007)



Thermoelectric materials for energy harvesting

A defining characteristic of an efficient TE material is its ZT (figure of merit)



$$ZT = \frac{S^2 \sigma}{k} T$$

S = Seebeck coefficient
 σ = electrical conductivity
 k = thermal conductivity
 T = absolute temperature

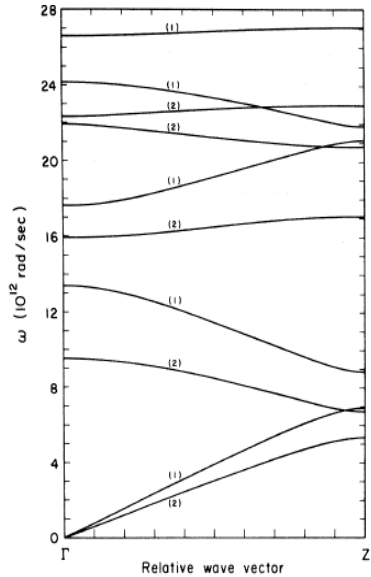
Traditional high ZT materials

Maximum power output: $1\text{-}2 \text{ mW/mm}^2$

Minnich et al. (Energy Environ. Sci, 2, 2009)

Future Direction:

- Next generation high ZT materials can be realized by **significantly reducing thermal conductivity** while enhancing/maintaining electrical conductivity of existing systems
- *Heat energy harvesting in semiconductor chips*- explore **newer TE systems** compatible with IC fabrication requirements that have optimal S , k , σ .
- Work at a range of operating temperatures compatible with semiconductor chips, and characterized by high power densities (> 10 's mW/mm^2).



Phononic band structure of Bi_2Te_3

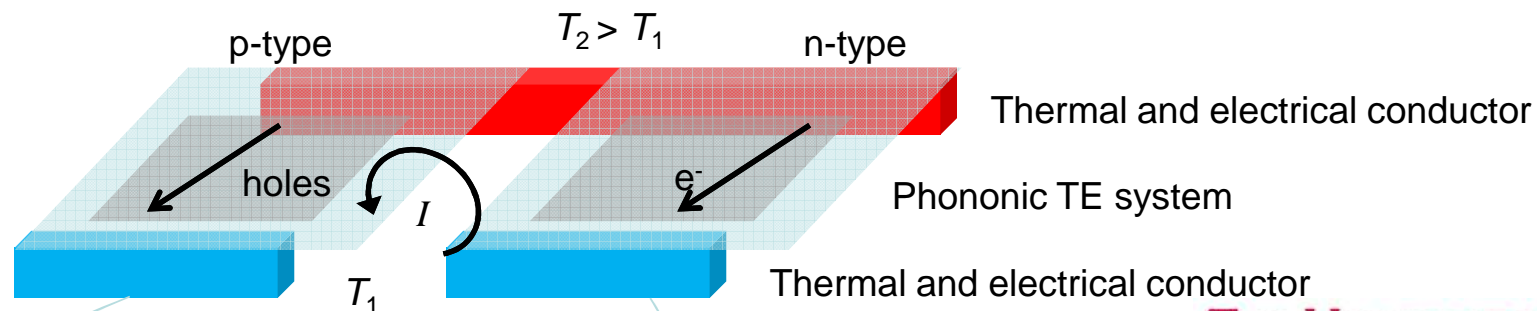
- High frequency 'non-thermal' phonons scatter charge carriers (electrons/holes)
- Acoustic (low frequency) phonons: responsible for thermal propagation (nanometric wavelengths)

ZT can be greatly enhanced if

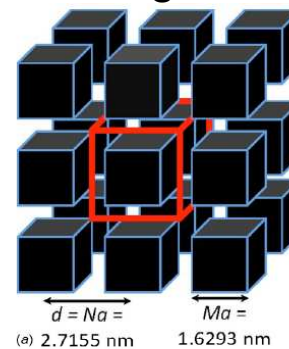
- thermal phonon transport is reduced (via introduction of band-gaps), without affecting electrical conductivity
- electron/hole transport is increased (by non-thermal phonon drag)

Phononic band structures of metamaterials can be modified based on **size, periodicity and properties of the secondary phase** (*inclusions, pores*)- the inclusions /pores should be of 10's of nanometers to achieve low-frequency band-gaps.

Non-thermal, high-frequency phonon transport (leading to phonon-drag), is achieved by introducing negative bands at high frequencies (*Bucay et al., Phys. Rev. B, 2009*)

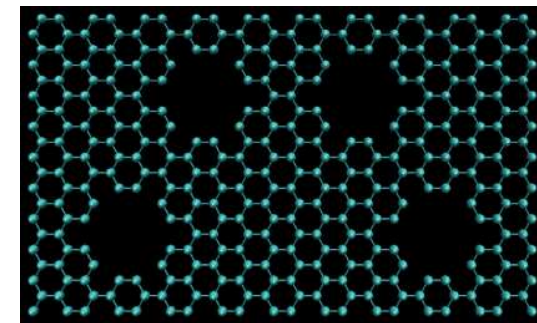
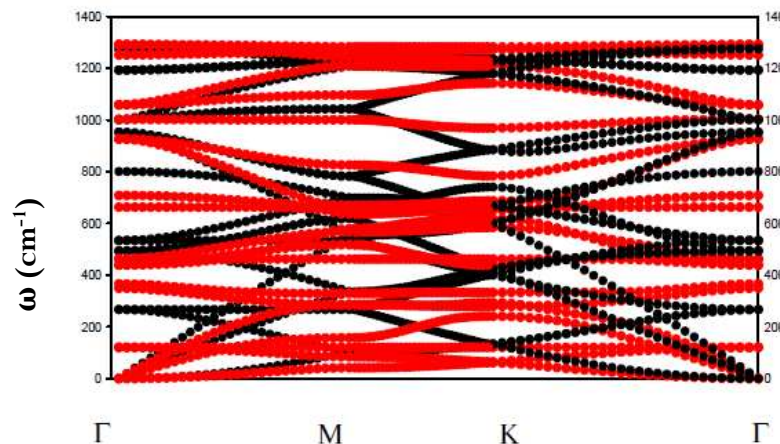


- **SiGe: superlattices, 3D nanostructures:** computational work by Gillet et al. (*J. heat transfer*, 131, 2009) has shown that the thermal conductivity can be reduced by two orders of magnitude for 3D nanostructure given below



Nanoscale Ge inclusions in a Si matrix.

- **Single layer and multilayer patterned graphene:** preliminary work has shown that low-frequency band-gaps are introduced in graphene nano-antidots



Other systems examined:

- Nanoporous silicon
- GaAs

Acknowledgements

- P. Deymier, J-F Robillard, W. Beck, J. Bucay, Univ. of Arizona
- D. Barker, Raytheon
- 3M Corporation
- J.O. Vasseur, Univ. Lille, France
- J. Page, A. Sukhovich, Univ. Manitoba Canada